Hepatitis C virus infection triggers a tumor-like glutamine metabolism

Pierre L. Lévy[1], Sarah Duponchel[1,2], Hannah Eischeid[3], Jennifer Molle[1], Maud Michelet[1], Gaëlle Diserens[4], Martina Vermathen[5], Peter Vermathen[4], Jean-Francois Dufour[4], Hans-Peter Dienes[3,6], Hans-Michael Steffen[3], Margarete Odenthal[3], Fabien Zoulim [1,2], Birke Bartosch[1]

[1]Cancer Research Center Lyon, INSERM U1052 and CNRS 5286, Lyon University, 69003 Lyon, France

[2] Hospices Civils de Lyon, France

[3]Institute of Pathology, University of Cologne, Germany

[4]Dept. of Clinical Research, University of Bern, Bern, Switzerland

[5]Dept. of Chemistry and Biochemistry, University of Bern, Bern, Switzerland

[6]Clinical Institute of Pathology, Medical University of Vienna, Austria

Keywords: chronic hepatitis C, glutaminolysis, fibrosis, hepatocarcinogenesis

This article has been accepted for publication and undergone full peer review but has not been through the copyediting, typesetting, pagination and proofreading process which may lead to differences between this version and the Version of Record. Please cite this article as doi: 10.1002/hep.28949

Contact information: Birke Bartosch, Cancer Research Center Lyon, 151 cours Albert Thomas, 69434 Lyon, France; Birke.Bartosch@inserm.fr, Tel 0033472681975, Fax 0033472681971

List of abbreviations: Hepatitis C virus (HCV), hepatocellular carcinoma (HCC), direct antiviral agents (DAA), sustained virological response (SVR), insulin resistance (IR), adenosine triphosphate (ATP), glutaminase (GLS), α-ketoglutarate (αKG), primary human hepatocytes (PHH), solute carrier family (SLC), non-essential amino acids (NEAA), body mass index (BMI), alkaline phosphatase (AP), aspartate aminotransferase (ASAT), alanine aminotransferase (ALAT), gamma-glutamyltransferase (GGT), albumin (Alb)

Financial support: French National Agency for AIDS and Viral Hepatitis Research (14370), Ligue contre le cancer Comité de Savoie, Agence Nationale de Recherche, DevWeCan French Laboratories of Excellence (ANR-10-LABX-61), OpeRa IHU program (ANR-10-IBHU-004)

Abstract

Chronic infection with hepatitis C virus (HCV) is one of the main causes of hepatocellular carcinoma. However, the molecular mechanisms linking the infection to cancer development remain poorly understood. Here we used HCV-infected cells and liver biopsies to study how HCV modulates the glutaminolysis pathway, which is known to play an important role in cellular energetics, stress defense and neoplastic transformation. Transcript levels of glutaminolytic factors were quantified in Huh7.5 cells or primary human hepatocytes infected with the JFH1 HCV strain as well as in biopsies of chronic HCV patients. Nutrient deprivation, biochemical analysis and metabolite quantification were performed with JFH1 infected Huh7.5 cells. Furthermore, shRNA vectors and small molecule inhibitors were used to investigate the dependence of HCV replication on metabolic changes. We show that HCV modulates the transcript levels of key enzymes of the glutamine metabolism *in vitro* and in liver biopsies of chronic HCV patients. Consistently, HCV infection increases glutamine utilization and dependence. We finally show that inhibiting glutamine metabolism attenuates HCV infection and the oxidative stress associated with HCV infection.

Conclusions:

Our data suggest that HCV establishes glutamine dependence, which is required for viral replication. Importantly, glutamine addiction is also a hallmark of tumor cells. While HCV induces glutaminolysis to create an environment favorable for viral replication, it predisposes the cell to transformation. Glutaminolytic enzymes may be interesting therapeutic targets for prevention of hepatocarcinogenesis in chronic hepatitis C.

Introduction

Over 170 million people are chronically infected with hepatitis C virus (HCV) worldwide, placing them at risk to develop chronic liver inflammation and fibrosis and to progress to cirrhosis and hepatocellular carcinoma (HCC) on the long term. Incidences of HCV-induced liver disease and cancer will remain high in the coming decade albeit recent progress in the development of direct antiviral agents (DAA) (1). With new treatments, sustained virological response (SVR) is predicted to become attainable for most patients (2). A therapeutically obtained SVR improves inflammation and fibrosis and decreases the risk for HCC. However, in up to 12% of SVR patients, fibrosis levels do not reverse and even progress to cirrhosis (3). Furthermore, HCC can still occur in SVR patients, even at long periods after treatment, and an advanced pretreatment fibrosis stage is considered a risk factor (4). Among the risk factors for fibrosis progression in chronic hepatitis C are features of the metabolic syndrome including obesity, dyslipidemia, insulin resistance (IR) and type 2 diabetes. Among these, IR and steatosis are frequent in patients and suspected – at least partially – to be directly induced by the virus (5, 6). However, metabolic fluxes in HCV-infected cells have not been analyzed in detail, despite their pivotal role in cellular transformation.

The predominant nutrient sources for cancer cells are glucose and glutamine. Both provide bioenergetics (ATP) and intermediates for macromolecular synthesis. So far only few reports have described changes to glucose uptake and utilization in HCV infection, moreover with contradictory results (7, 8). Altered glucose utilization with augmented lactate production and glutamine uptake have been reported in HCV-infected hepatoma cells (8, 9), but no underlying details have been published. Glutamine supports many metabolic functions needed for cell survival, growth and proliferation. In particular it serves as precursor for other amino acids, nucleotides and lipids and as substrate for oxidative phosphorylation. In addition it is required for glutathione synthesis and redox homeostasis (10). Glutaminolysis is initiated by the conversion of glutamine to glutamate, catalyzed by the rate-limiting enzyme glutaminase (GLS). Glutamate can serve as precursor for nucleic acid and serine synthesis, drives the uptake of other amino acids or is further converted by glutamate-dehydrogenase or transaminases to α-ketoglutarate (αKG), which enters the TCA cycle. The phenomenon of glutamine-driven anaplerosis provides biosynthetic precursors and allows many tumor cells to sustain ATP production by providing enough reducing equivalents to the electron transport chain (11). Two

human glutaminase genes exist, *GLS* (*GLS1*) and *GLS2*. *GLS* displays oncogenic activity while the potential role of *GLS2* in cancer remains less clear (12). Two *GLS* isoforms have been described, termed KGA and GAC, but their respective functional differences remain uncharacterized.

Given the importance of glutamine in carcinogenesis, we investigated the role of glutaminolysis in HCV infection. We show that HCV increases expression of glutaminolytic enzymes, glutamine uptake and glutamine utilization in *in vitro* infected Huh7.5 cell cultures. Transcripts of key glutaminolytic genes were also increased by HCV in infected primary human hepatocytes (PHH). Importantly, we show using GLS specific pharmacological inhibitors that HCV replication is sensitive to glutaminolysis. Furthermore, expression of several glutaminolytic genes increased together with fibrosis stage and inflammation grade in HCV-liver biopsies. Our results suggest that HCV stimulates the glutamine metabolism, a metabolic adaptation that boosts viral replication and that may play an important role in the predisposition to HCC in chronically infected patients.

Experimental procedures

Cell culture

Huh7.5 cells were maintained in Dulbecco's Modified Eagle Medium containing 25 mM glucose, 1X GlutaMAX, 100 U/mL penicillin and 100 µg/mL streptomycin (Life Technologies) and 10% FCS (Thermo Scientific), in a 5% CO2-normoxia incubator at 37°C. For glucose and glutamine titration and deprivation experiments, Huh7.5 cells were cultured in DMEM no glucose, no glutamine supplemented or not with 25 mM glucose and 2 mM glutamine, 100 U/mL penicillin, 100 µg/mL streptomycin and 10% dialyzed FCS (Life Technologies).

HCVcc production

The HCV JFH1 strain previously described by Delgrange et al. (13) was *in vitro* transcribed and electroporated into Huh7.5 cells. Supernatants were harvested, filtered (0.45 µm) and used to infect naive Huh7.5 cells. Pooled supernatants were quantified using the $TCID_{50}$ method.

Glucose/glutamine utilization and lactate production measurements

Glucose, glutamine and lactate were quantified by calculating the difference in concentration between the culture medium after 24h culture. Glucose titration reagent contained 0,1M

triethanolamine pH 7.5 (Sigma), 2 mM $NADP^+$ (Roche), 2 mM ATP (Sigma), 2 u/ml hexokinase (Sigma) and 2 u/ml glucose-6-phosphate dehydrogenase (Roche). Glutamine was quantified using the L-Glutamine/Ammonia assay kit (Megazyme), glutamate with Glutamate Assay Kit (Abcam) and glutaminase activity with Glutaminase Microplate Assay Kit (Cohesion biosciences). Lactate titration reagent contained hydrazine/glycine (0.4/0.5M) pH 9 (Sigma), 2 mM NAD^+ (Sigma) and 2 u/ml lactate dehydrogenase (Sigma). NADH or NADPH production was quantified by measuring the end-point OD of reactions at 340 nm.

Liver biopsies

Liver biopsies from control (Hodgkin's lymphoma, n=12) and chronic hepatitis C (n=119) patients and paired biopsies from chronic hepatitis C patients before and during α-interferon/ribavirin treatment were acquired during routine diagnostic work whenever sufficient material was available. Information on HCV genotype was available for 77 patients, 49 were infected with genotype 1 and 28 with genotype 2. Biopsies were used under the French IRB "Comité de Protection des Personnes Sud-Est 287 IV" agreement #11/040 obtained in 2011. Written informed consent had been obtained.

RT-qPCR

RNA was extracted from cells with Trizol reagent (Life Technologies). 1 µg of total RNA was DNase-treated (Roche) and reverse transcribed (M-MLV RT, Life Technologies). RNA from liver biopsy samples was purified (Nucleospin RNA/protein kit, Macherey-Nagel). 350 ng of RNA was reverse transcribed (Superscript Vilo enzyme, Life Technologies). Transcript levels of target genes were quantified by RT-qPCR using Sybr Green I Master Mix (Roche) on a LightCycler 480 (Roche). Glucuronidase beta (*GUSB*) served as reference gene for the *in vitro* study and phosphomannomutase 1 (*PMM1*) for liver biopsies. All primers sequences are available upon request. For JFH1, specific primers were adapted from the RC1 and RC21 primers (14).

Statistics

Statistics were performed with Student's t test or the non-parametric Mann-Whitney U and Wilcoxon signed rank tests and Spearman correlation analysis. p-value *: < 0.05; **: < 0.01; ***: < 0.001; ****: < 0,0001

Additional methods are described in the supplementary section.

Results

HCV infection up-regulates several key factors of glutamine metabolism

Basal transcript levels of glutaminolytic factors were compared in Huh7.5 cells and PHH. MYC is a key transcription factor that drives glutamine addiction in cancer cells by inducing the transcription of various glutamine transporters such as Solute carrier family 1 member 5 (SLC1A5) and SLC7A5 as well as of GLS, the rate-limiting enzyme of glutaminolysis. Overall, transcript levels of these genes were lower in PHH compared to Huh7.5 cells, likely due to the transformed background of the hepatoma cell line (Figure 1A). Albeit elevated baseline levels of transcripts of glutaminolytic factors in Huh7.5 cells, HCV increased mRNA levels of *MYC* and both glutaminase transporters significantly not only in PHH but also in Huh7.5 cells, infected at a multiplicity of infection (MOI) of 5 and 1, respectively. (Figure 1B,C). HCV also induced the two *GLS* isoforms KGA and GAC in Huh7.5 cells, while only *GLS* GAC was found increased in PHH. Both isoforms are associated with carcinogenesis. In contrast, HCV did not induce transcript levels of *GLS2*, the isoform expressed in the liver under normal physiological conditions, in Huh7.5 nor in PHH. Induction of glutaminolytic transcripts was not observed with UV-irradiated virus (Figure 1C), and induction of MYC and GLS by naïve virus confirmed on the protein level in Huh7.5 cells (Figure 1D). In infected cells, MYC accumulated particularly in nuclear fractions, indicating activation of its transcriptional activity. In order to test whether induction of glutaminolytic factors by the virus is a direct effect, co-localizations were performed on infected Huh7.5 cells (MOI 0,1) at 3 days post infection (dpi), using an antibody specific to GLS isoforms KGA and GAC. The virus was present in a large majority of cells, but expression levels were heterogeneous. GLS expression was overall induced by the virus in the culture, but strongly HCV-positive cells did not display the highest GLS staining (Figure 1E), suggesting that GLS induction may not be directly mediated by HCV but rather by virus-induced oxidative stress or inflammatory processes. GLS induction by HCV was furthermore found to be reversible. Huh7.5 cells were infected at an MOI of 0,1 for 4 days and then treated with the DAA sofosbuvir for further 2 days (Figure 1F). mRNA levels of *MYC, GLS KGA and GAC, SLC1A5* and *SLC7A5* were increased in cultures 4 dpi, but returned to baseline upon successful elimination of HCV by sofosbuvir treatment, demonstrating that the transcriptional induction of these genes is reversible.

Glutamine metabolization is increased in HCV-infected cells

The effect of HCV on glucose and glutamine utilization was assessed. 3 dpi, when the virus had spread throughout the culture (Figure 2A), culture medium was changed and harvested 24hrs later to quantitate glucose and glutamine. In infected cells, consumption of both nutrients was increased (Figure 2B), suggesting that HCV induces glycolysis as well as glutaminolysis. To test the impact of nutrient composition of the culture medium on HCV-induced glutamine uptake, mock and infected cells were cultured from 3 dpi onwards in conditioned media containing glucose or glutamine only, or the combination. Supernatants were harvested 24hrs later, and the procedure repeated on day 4 and 5. Supernatants were analyzed by nuclear magnetic resonance (NMR). HCV induced significant changes to levels of several amino acids. However, only glutamine and glutamate levels were changed in mock versus infected cells irrespective of the culture media used (Table 1, Figure 2C). Infected cells depleted more glutamine compared to mock from the supernatant, while glutamate levels increased, pointing to an active glutamate export from infected cells, possibly in exchange for other amino acids. In order to ask whether glutamine taken up by infected cells feeds into the TCA cycle, and in order to assess the respective contributions of glutaminolysis and glycolysis to the TCA cycle, lactate production was quantified. Glucose is the predominant substrate for lactate production. However, lactate can also be produced from glutamine via the TCA cycle intermediate malate. 3 dpi cell media were replaced with conditioned media containing both glucose and glutamine, glutamine only or glucose only and were harvested 24hrs later. In the presence of glucose containing media, HCV increased lactate production by 20 to 30% (Figure 2D). When only glutamine was available overall lactate production was lower, but HCV increased lactate production by close to 300%, indicating that partial glutamine oxidation through the TCA cycle is significantly activated in HCV-infected cells. These data were confirmed in a 3 day time course in medium containing glutamine only, where lactate production increased over time (Figure 2E).

Glutamine is more essential than glucose for the proliferation of HCV-infected cells

To estimate the relative importance of glucose and glutamine in HCV infection, proliferation of mock and HCV-infected cells was monitored in conditioned media containing or not glucose and glutamine. HCV-infected Huh7.5 cells were seeded and cultured in the indicated growth media and cell proliferation quantified each day. Proliferation of control cells was overall faster than that of HCV-infected cells and more sensitive to glucose than to glutamine deprivation. In contrast, proliferation of HCV-infected cells was more sensitive to glutamine than to glucose withdrawal, underlining the importance of glutamine in HCV infected cells (Figure 3A,B). HCV expression was still detectable under all culture conditions 4 days after medium change (Figure 3C,D), suggesting that the differences in proliferation were predominantly due to metabolic restraints induced by the virus. Furthermore, the effects of glutamine withdrawal on proliferation of both mock and HCV-infected cells could be almost completely rescued by αKG supplementation (Figure 3A, B), suggesting that HCV induces glutaminolysis in order to maintain TCA cycle activity.

Glutaminolysis is required for HCV replication

To investigate the dependence of HCV on glutamine metabolism, Huh7.5 cells were infected and culture media changed 4hrs later with control and glutamine-deprived media. Viral RNA was quantified by RT-qPCR 3 dpi and standardized to cellular RNA content in order to compensate for effects on cell growth (Figure 4A). Glutamine withdrawal from cell culture medium clearly inhibited the establishment of an HCV infection by over 60%. Addition of non-essential amino acids (NEAA), glutamate or αKG to the no-glutamine medium rescued HCV replication (Figure 4A). This indicates that HCV requires glutamine for production of αKG, likely for anaplerotic purposes. To verify the importance of glutaminolysis in the HCV life cycle, transcript levels of *MYC* and *GLS* were silenced in Huh7.5 cells with shRNAs. Knock down efficiencies of the shRNAs were verified the same day the cells were seeded for infection. *MYC* and *GLS* transcript levels were found to be reduced by 67% and 71%, respectively in comparison to control shRNA (Figure 4B). 3 dpi HCV replication was quantified and found to be inhibited by 53 and 38% in shMYC and shGLS cells, respectively, compared to scramble control. Silencing of *GLS* could be partially rescued by addition of αKG. To validate MYC and GLS as antiviral targets, the effect of pharmacological small molecule inhibitors on HCV replication was tested. The MYC inhibitor 10058-F4 is known to have a potent anti-cancer effect *in vitro* (15). The GLS inhibitors [Bis-2-(5-phenylacetamido-1,3,4-thiadiazol-2-yl)ethyl sulfide (BPTES) and CB-839 are known to block the catalytic center of GLS. CB-839 is currently under evaluation in a phase I clinical

trial for several types of cancers (16, 17). No cell toxicity of these inhibitors was observed on Huh7.5 cells with the exception of CB-839 where cytotoxicity became detectable at the strongest dose tested (Figure 4C). Huh7.5 cells were infected with MOIs of 0,1 and 1, the inhibitors or carrier added 4 hrs later and replication quantitated 3 dpi. All three molecules inhibited the establishment of an infection in a dose dependent fashion with the strongest effect displayed by CB-839 (Figure 4C). CB-839 treatment also reduced HCV NS3 and NS5A protein levels at 3 dpi (Figure 4D). To control the pharmacological inhibition of GLS activity, intracellular glutamate levels as well as glutaminase activity were assessed in the presence of CB-839. HCV increased glutaminase activity in infected cells by ca 1,5 fold (Figure 4D). This increase was inhibited in a dose dependent manner by CB-839. Intracellular glutamate levels were not increased by the virus, possibly due to the important turn over and utilization of glutamate for amino acid import/exchange and the TCA cycle, as shown before in Figure 2C and D. CB-839, however, decreased intracellular glutamate in a dose dependent fashion (Figure 4D). The antiviral effect of CB-839 could be partially reversed by addition of αKG, suggesting that besides an increased glutaminolytic flux into the Krebs cycle glutaminase may fulfill additional functions in the viral life cycle (Figure 4D). To investigate whether the pharmacological inhibitors of MYC and GLS also inhibit an already established infection, Huh7.5 cells were infected and cultured for a minimum of 10 days. Infected cells were re-seeded, 10058-F4, CB-839 or DMSO carrier added and HCV replication quantified 3 days later. Inhibition of MYC had a reproducible, moderate inhibitory effect. Inhibition of GLS blocked HCV replication in a dose dependent manner by up to 40% within the 3 day period (Figure 4E).

HCV has previously been shown to augment production of oxidative stress and in particular superoxide anions (18). In addition, glutaminolysis in cancer cells is required for redox homeostasis. Therefore the effect of CB-839 on superoxide anion levels in HCV infected cells was assessed. CB-839 partially blocked the 2 fold increase of superoxide anions induced by HCV (Figure 4F).

MYC, SLC7A5 and GLS levels are elevated in chronic hepatitis C patients

To explore whether glutaminolysis is induced *in vivo*, *MYC*, *SLC1A5*, *SLC7A5* and *GLS* (KGA and GAC) transcript levels were quantified by RT-qPCR in liver biopsies from patients with chronic hepatitis C (n = 119) diagnosed with genotype 1 or 2, as well as patients with liver complications from Hodgkin's lymphoma as control (n = 12). No difference in the transcript levels of *SLC1A5* was

detected. However, mRNA levels of *MYC, SLC7A5* and both *GLS* isoforms were significantly elevated in the HCV group (Figure 5A). Among the HCV patient cohort, activity grades and fibrosis stages were available for 117/119 and 101/119 biopsies, respectively. *MYC, SLC1A5* and *GLS* (KGA and GAC) mRNA levels increased together with activity grade and fibrosis stage (Figure 5A). Additional clinical data could be obtained for some of the HCV patients: age (for 90/119 patients); body mass index (BMI) (65/119); alkaline phosphatase (77/119); aspartate aminotransferase (ASAT) (78/119); alanine aminotransferase (ALAT) (78/119); gamma-glutamyltransferase (GGT) (78/119); albumin (67/119). Results of association studies are presented in Table 2. Weak but significant positive correlations were detected between *MYC*, *SLC1A5, GLS* KGA, *GLS* GAC and GGT and ASAT levels; further correlations were found between *GLS* KGA, *GLS* GAC and BMI as well as between *GLS* GAC and ALAT levels. Furthermore a tendency for a correlation between *MYC*, *SLC1A5* and *GLS* KGA mRNA and ALAT levels (p-values between 0.0575 and 0.0708) was observed. No difference between the transcript levels of all these genes between patients infected with HCV genotype 1 and 2 was observed (not shown), suggesting that induction of glutaminolysis is induced in the context of both genotypes. To ask whether increases in *MYC*, *SLC7A5* and *GLS* levels in patients were virus-induced and reversible upon antiviral treatment, transcripts of HCV, *MYC*, *SLC1A5*, *SLC7A5* and *GLS* were quantified in 9 paired biopsy couples obtained from patients before and during/after α-interferon/ribavirin treatment (Figure 5B). *MYC* and *SLC7A5* were significantly decreased with antiviral treatment alongside HCV levels. GLS levels showed a tendency to decrease (p=0.13) and no difference in transcript levels was observed for *SLC1A5*.

Discussion

The molecular mechanisms involved in the progression from chronic HCV infection to HCC are not well established. Here, we report that HCV infection may predispose hepatocytes to liver tumorigenesis through alterations of glutamine metabolism (Figure 6). In tumor cells glutamine utilization and the subsequent induction of key target genes involved in glutamine uptake and oxidation is frequently driven by the transcription factor MYC (19). Induction of MYC expression by HCV-induced beta catenin and -Akt signaling has already been reported (20, 21), but we have extended this finding to MYC-target genes that drive glutamine metabolism: the two glutamine

transporters *SLC1A5* and *SLC7A5*, as well as two cancer-associated isoforms of glutaminase - *GLS KGA* and *GAC*. Even though basal expression of glutaminolytic factors is elevated in Huh7.5 cells in comparison to PHH, HCV still induces a significant additional increase of these factors in this cell line. We therefore based our experimental approaches on Huh7.5 cells and corroborated these findings in a physiologically appropriate background including experimentally infected PHH and liver biopsies of HCV infected patients.

Interestingly, SLC1A5 and SLC7A5 have been described in the literature to be up-regulated in a broad range of human cancers, including HCC (22). Likewise, high expression and activity of GLS *KGA* and *GAC* in cancer cells have been extensively reported (10, 23). GLS is known to be important for liver cancer. Indeed, GLS activity is known to correlate with the volume doubling time of rat hepatomas (24). Here, we observed that HCV infection increased the transcripts of both *KGA* and *GAC* isoforms to a similar extent in Huh7.5 cells, however only the *KGA* isoform was found induced by HCV in PHH, while both *KGA* and *GAC* isoforms were induced in patient biopsies. The reasons for this discrepant finding are unclear at this stage and warrant further investigation. Transcript levels of *GLS2*, the glutaminase endogenously expressed in the liver, were at the limit of detection in Huh7.5 cells and not increased by the virus in Huh7.5 cells nor in PHH. In addition, we observed increased glutamine consumption in HCV-infected Huh7.5 cells together with an elevation of glucose utilization and lactate production. These results are consistent with the recently reported stabilization of hypoxia inducible factor 1α, the increase of hexokinase 2 activity and stimulation of aerobic glycolysis in infected cells (8, 25). Furthermore, the cancer specific form of pyruvate kinase, PKM2, which mediates the final step of glycolysis, has been shown to interact with HCV polymerase NS5B and to be required for HCV replication (26, 27). These data, as well as a recent proteomic analysis of HCV-infected cells (9), suggest that glycolysis plays a major role in the HCV life cycle.

A frequent consequence of aerobic glycolysis is the inhibition of glucose-derived pyruvate entry in the mitochondria, where the TCA cycle produces precursors for biosynthetic processes such as lipid, nucleotide and amino acid synthesis. Tumor cells are known to compensate for the loss of glucose-derived TCA cycle intermediates by activating glutaminolysis (10). Our results strongly suggest that HCV reprograms metabolism by increasing utilization of glutamine for anaplerotic purposes. However, a part of the absorbed glutamine is re-secreted in the form of glutamate, probably in exchange for other amino acids. This finding has already been reported in various cancer cells and confirms an

important role for the amino acid metabolism in HCV infection (28). The deleterious effects of glutamine withdrawal on the growth of HCV-infected cells could be fully rescued by αKG. Increased glutaminolysis and TCA cycle activity have been associated with increased respiratory activity and production of reactive oxygen species in cancer cells. The glutaminase inhibitor CB-839 partially reduced the HCV-induced increase of superoxide anion production in Huh7.5 cells, suggesting that at least in part the increase in oxidative stress in infected cells is due to mitochondrial/respiratory activity. Therefore it will be interesting to investigate whether glutaminase inhibitors reduce the oxidative and inflammatory environment that contributes to fibrosis progression in the infected liver. Furthermore, we found that early glutamine withdrawal after HCV infection inhibited viral replication. Again, the reason is likely to be a drop in TCA cycle intermediates as the effect could be rescued by αKG supplementation, however the rescue was less efficient than rescue in the context of Gln withdrawal or GLS silencing for reasons that warrant further investigation.

It was recently shown that reductive carboxylation of glutamine-derived αKG was the predominant source of *de novo* lipid synthesis in many tumor cells (29-31). Considering the importance of lipids in the HCV life cycle (6), reductive carboxylation from glutamine-derived carbons may be activated in HCV-infected cells to provide lipids in favor of the HCV life cycle. Further experiments are required to verify this hypothesis. In the present study, targeting MYC or GLS, via shRNA or pharmacological inhibitors, significantly attenuated HCV replication. Considering the major functions of MYC in the promotion of cell growth, many pathways are likely to be deregulated by its inhibition. However, targeting GLS more specifically suppresses glutaminolysis, which strengthens the important role of this pathway in HCV replication. Interestingly, glutaminase inhibitors have recently also been shown to display antiviral activity against adenovirus, herpes simplex virus 1 and influenza A (32), suggesting that glutaminase inhibitors may be interesting to develop as general antivirals because they block the metabolic requirements for progeny virion production.

The importance of glutaminolysis in HCV replication *in vitro* was validated *in vivo* in HCV liver biopsies. MYC, SLC7A5 and both forms of GLS were increased in biopsies of HCV-infected patients compared to control liver biopsies derived from Hodgkin's lymphoma, that are characterized by hepatic infiltrations. Transcripts of glutaminolytic factors tended to decrease upon antiviral treatment, suggesting that glutaminolysis is at least partially reversible *in vivo*. Moreover, transcript levels of MYC, SLC1A5 and both forms of GLS progressively increased together with fibrosis stage, activity

grade, and serum levels of several liver enzymes. These data suggest, that although some direct effects of HCV are likely to participate, oxidative stress, inflammation and liver disease may also be linked to and amplify the increase of glutaminolysis. The possibility of an indirect induction of glutaminolysis by HCV is furthermore supported by our finding that the levels of GLS expression did not always correlate with HCV protein levels in *in vitro* infected Huh7.5 cells. Surprisingly few is known so far on the links between glutaminolysis, oxidative stress and immune reactions, however, an increase in hepatic glutamine transport has been associated with inflammation in a model of endotoxemic rats (33). In contrast to the other glutaminolytic factors, SLC7A5 levels were already higher in HCV patients with low or no liver damage and did not increase further with activity grade, nor with the fibrosis stage. Interestingly, SLC7A5 is necessary for mTOR activation, a factor that is induced in up to 50% of HCCs (34) and been shown to be required for HCV replication (28, 35, 36).

Collectively, our data revealed for the first time a link between HCV infection and glutaminolysis. We show that viral replication depends on glutaminolysis using genetic and pharmacological approaches. Importantly, increased levels of glutaminolysis are likely to provide a metabolic environment in infected cells that predisposes to and favors the development of HCC. Thus, glutaminolysis inhibitors, currently in clinical trials for cancer treatment, may prove useful for prevention of fibrosis progression and cellular transformation particularly in patients at risk of disease progression towards HCC despite viral elimination with the newly available DAAs.

References

1. Thomas DL. Global control of hepatitis C: where challenge meets opportunity. Nat Med 2013;19:850-858.

2. Pawlotsky JM. New hepatitis C therapies: the toolbox, strategies, and challenges. Gastroenterology 2014;146:1176-1192.

3. Lee YA, Friedman SL. Reversal, maintenance or progression: what happens to the liver after a virologic cure of hepatitis C? Antiviral Res 2014;107:23-30.

4. Yamashita N, Ohho A, Yamasaki A, Kurokawa M, Kotoh K, Kajiwara E. Hepatocarcinogenesis in chronic hepatitis C patients achieving a sustained virological response to interferon: significance of lifelong periodic cancer screening for improving outcomes. J Gastroenterol 2013.

5. Kaddai V, Negro F. Current understanding of insulin resistance in hepatitis C. Expert Rev Gastroenterol Hepatol 2011;5:503-516.

6. Negro F. Abnormalities of lipid metabolism in hepatitis C virus infection. Gut 2010;59:1279-1287.

7. Kasai D, Adachi T, Deng L, Nagano-Fujii M, Sada K, Ikeda M, Kato N, et al. HCV replication suppresses cellular glucose uptake through down-regulation of cell surface expression of glucose transporters. J Hepatol 2009;50:883-894.

8. Ramiere C, Rodriguez J, Enache LS, Lotteau V, Andre P, Diaz O. Activity of hexokinase is increased by its interaction with hepatitis C virus protein NS5A. J Virol 2014;88:3246-3254.

9. Diamond DL, Syder AJ, Jacobs JM, Sorensen CM, Walters KA, Proll SC, McDermott JE, et al. Temporal proteome and lipidome profiles reveal hepatitis C virus-associated reprogramming of hepatocellular metabolism and bioenergetics. PLoS Pathog 2010;6:e1000719.

10. DeBerardinis RJ, Cheng T. Q's next: the diverse functions of glutamine in metabolism, cell biology and cancer. Oncogene 2010;29:313-324.

11. Fan J, Kamphorst JJ, Mathew R, Chung MK, White E, Shlomi T, Rabinowitz JD. Glutamine-driven oxidative phosphorylation is a major ATP source in transformed mammalian cells in both normoxia and hypoxia. Mol Syst Biol 2013;9:712.

12. Cassago A, Ferreira AP, Ferreira IM, Fornezari C, Gomes ER, Greene KS, Pereira HM, et al. Mitochondrial localization and structure-based phosphate activation mechanism of Glutaminase C with implications for cancer metabolism. Proc Natl Acad Sci U S A 2012;109:1092-1097.

13. Delgrange D, Pillez A, Castelain S, Cocquerel L, Rouille Y, Dubuisson J, Wakita T, et al. Robust production of infectious viral particles in Huh-7 cells by introducing mutations in hepatitis C virus structural proteins. J Gen Virol 2007;88:2495-2503.

14. Komurian-Pradel F, Perret M, Deiman B, Sodoyer M, Lotteau V, Paranhos-Baccala G, Andre P. Strand specific quantitative real-time PCR to study replication of hepatitis C virus genome. J Virol Methods 2004;116:103-106.

15. Gomez-Curet I, Perkins RS, Bennett R, Feidler KL, Dunn SP, Krueger LJ. c-Myc inhibition negatively impacts lymphoma growth. J Pediatr Surg 2006;41:207-211; discussion 207-211.

16. Robinson MM, McBryant SJ, Tsukamoto T, Rojas C, Ferraris DV, Hamilton SK, Hansen JC, et al. Novel mechanism of inhibition of rat kidney-type glutaminase by bis-2-(5-phenylacetamido-1,2,4-thiadiazol-2-yl)ethyl sulfide (BPTES). Biochem J 2007;406:407-414.

17. Gross MI, Demo SD, Dennison JB, Chen L, Chernov-Rogan T, Goyal B, Janes JR, et al. Antitumor activity of the glutaminase inhibitor CB-839 in triple-negative breast cancer. Mol Cancer Ther 2014;13:890-901.

18. Brault C, Levy P, Duponchel S, Michelet M, Salle A, Pecheur EI, Plissonnier ML, et al. Glutathione peroxidase 4 is reversibly induced by HCV to control lipid peroxidation and to increase virion infectivity. Gut 2014.

19. Dang CV. MYC, metabolism, cell growth, and tumorigenesis. Cold Spring Harb Perspect Med 2013;3.

20. Colman H, Le Berre-Scoul C, Hernandez C, Pierredon S, Bihouee A, Houlgatte R, Vagner S, et al. Genome-wide analysis of host mRNA translation during hepatitis C virus infection. J Virol 2013;87:6668-6677.

21. Higgs MR, Lerat H, Pawlotsky JM. Hepatitis C virus-induced activation of beta-catenin promotes c-Myc expression and a cascade of pro-carcinogenetic events. Oncogene 2013;32:4683-4693.

22. Fuchs BC, Bode BP. Amino acid transporters ASCT2 and LAT1 in cancer: partners in crime? Semin Cancer Biol 2005;15:254-266.

23. Souba WW. Glutamine and cancer. Ann Surg 1993;218:715-728.

24. Knox WE, Horowitz ML, Friedell GH. The proportionality of glutaminase content to growth rate and morphology of rat neoplasms. Cancer Res 1969;29:669-680.

25. Wilson GK, Brimacombe CL, Rowe IA, Reynolds GM, Fletcher NF, Stamataki Z, Bhogal RH, et al. A dual role for hypoxia inducible factor-1alpha in the hepatitis C virus lifecycle and hepatoma migration. J Hepatol 2012;56:803-809.

26. Wu X, Zhou Y, Zhang K, Liu Q, Guo D. Isoform-specific interaction of pyruvate kinase with hepatitis C virus NS5B. FEBS Lett 2008;582:2155-2160.

27. Christofk HR, Vander Heiden MG, Harris MH, Ramanathan A, Gerszten RE, Wei R, Fleming MD, et al. The M2 splice isoform of pyruvate kinase is important for cancer metabolism and tumour growth. Nature 2008;452:230-233.

28. Stohr S, Costa R, Sandmann L, Westhaus S, Pfaender S, Anggakusuma, Dazert E, et al. Host cell mTORC1 is required for HCV RNA replication. Gut 2015.

29. Metallo CM, Gameiro PA, Bell EL, Mattaini KR, Yang J, Hiller K, Jewell CM, et al. Reductive glutamine metabolism by IDH1 mediates lipogenesis under hypoxia. Nature 2012;481:380-384.

30. Mullen AR, Wheaton WW, Jin ES, Chen PH, Sullivan LB, Cheng T, Yang Y, et al. Reductive carboxylation supports growth in tumour cells with defective mitochondria. Nature 2012;481:385-388.

31. Wise DR, Ward PS, Shay JE, Cross JR, Gruber JJ, Sachdeva UM, Platt JM, et al. Hypoxia promotes isocitrate dehydrogenase-dependent carboxylation of alpha-ketoglutarate to citrate to support cell growth and viability. Proc Natl Acad Sci U S A 2011;108:19611-19616.

32. Thai M, Thaker SK, Feng J, Du Y, Hu H, Ting Wu T, Graeber TG, et al. MYC-induced reprogramming of glutamine catabolism supports optimal virus replication. Nat Commun 2015;6:8873.

33. Karinch AM, Pan M, Lin CM, Strange R, Souba WW. Glutamine metabolism in sepsis and infection. J Nutr 2001;131:2535S-2538S; discussion 2550S-2531S.

34. Matter MS, Decaens T, Andersen JB, Thorgeirsson SS. Targeting the mTOR pathway in hepatocellular carcinoma: current state and future trends. J Hepatol 2014;60:855-865.

35. Csibi A, Lee G, Yoon SO, Tong H, Ilter D, Elia I, Fendt SM, et al. The mTORC1/S6K1 Pathway Regulates Glutamine Metabolism through the eIF4B-Dependent Control of c-Myc Translation. Curr Biol 2014;24:2274-2280.

36. Csibi A, Fendt SM, Li C, Poulogiannis G, Choo AY, Chapski DJ, Jeong SM, et al. The mTORC1 pathway stimulates glutamine metabolism and cell proliferation by repressing SIRT4. Cell 2013;153:840-854.

37. Cheng T, Sudderth J, Yang C, Mullen AR, Jin ES, Mates JM, DeBerardinis RJ. Pyruvate carboxylase is required for glutamine-independent growth of tumor cells. Proc Natl Acad Sci U S A 2011;108:8674-8679.

38. Popov N, Wanzel M, Madiredjo M, Zhang D, Beijersbergen R, Bernards R, Moll R, et al. The ubiquitin-specific protease USP28 is required for MYC stability. Nat Cell Biol 2007;9:765-774.

Figure Legends

Figure 1. Glutaminolytic factors are increased in HCV-infected cells and return to basal levels upon viral clearance

(A) Expression levels of MYC, SLC1A5, SLC7A5 and GLS isoforms KGA and GAC or GLS2 transcripts were quantified by RT-qPCR in Huh7.5 cells and primary human hepatocytes (PHH) using GUS as housekeeping gene (mean±SEM values of 3 or more independent experiments). **(B)** HCV replication levels at 3 dpi in Huh7.5 cells infected (MOI 1) with native or UV irradiated virus analyzed by RTqPCR and immunofluorescence (IF) with an anti-HCV serum (green). PHH infected with HCV at an MOI of 5 to 10 and harvested between 3 and 5 dpi (absolute quantification revealed between 4000 to 9000 HCV genome copies/µg RNA). **(C)** MYC, SLC1A5, SLC7A5, GLS KGA /GAC and GLS2 transcript levels were amplified using GUS as housekeeping gene in Huh7.5 cells and PHH. Fold changes standardized to mock infection are shown (mean±SEM, n= 2 to 10 independent experiments). **(D)** Total lysates, nuclear and cytoplasmic fractions of HCV infected Huh7.5 cells were immunoblotted with -MYC, -PARP, -Tubulin, -GLS, -actin and -core specific antibodies. Protein quantification was performed with ImageJ software. Results were standardized to PARP (MYC) or actin (GLS) expression and are expressed as fold change between infected and uninfected cells (a representative immunoblot is shown; graph: mean±SEM, n=4). **(E)** Huh7.5 cells were infected with HCV (MOI 0.1). 3 dpi, cells were fixed and stained with anti-HCV serum and anti-GLS antibody. Representative images are shown, n=4. **(F)** 4 dpi infected (MOI 0,1) and uninfected Huh7.5 cells were treated with 5 µM sofosbuvir (Sofo) or carrier for 2 days. HCV, MYC, SLC1A5, SLC7A5 and GLS mRNA levels were quantified by RT-qPCR at 4 and 6 dpi using GUS as housekeeping gene. HCV data were standardized to infection at 4 dpi. MYC, SLC1A5, SLC7A5 and GLS were standardized to mock-infection (mean±SEM, n=up to 7) **(C-F)** Statistics: Student *t*-test.

Figure 2. HCV infection increases glutamine utilization

(A–E) Huh7.5 cells were mock- or HCV-infected (MOI 1) for 3 days before cell media change. 24 hrs after the cell medium change, cell numbers were counted and supernatants harvested for metabolite quantification. Metabolite concentrations were corrected for cell numbers. Grey bars present mock, black bars HCV infected cultures. **(A)** HCV infection was controlled at 3 dpi by IF with an anti-HCV serum (green). **(B)** Glucose and glutamine consumption was measured biochemically in normal

medium (25mM glucose, 2mM glutamine) and data were standardized to mock infected cells. (mean±SEM, n=4) **(C)** Supernatants of mock and infected cells cultured in normal medium or conditioned media containing only glucose or only glutamine were harvested 3, 4 and 5 dpi and subjected to NMR analysis. Glutamine and glutamate concentrations (arbitrary units) were standardized for cell numbers. (mean±STD, n=3). **(D)** Lactate was quantified biochemically in supernatants of infected/uninfected cells cultured in the indicated conditioned cell media at 3 dpi. Data are standardized to mock infected cells cultured in normal medium (mean±SEM, n=4). **(E)** Lactate was quantified by NMR in supernatants of mock and infected cells cultured in only glutamine containing medium at 3, 4 and 5 dpi. Lactate concentrations (arbitrary units) were standardized for cell numbers. (mean±SEM, n=3).

Figure 3. Proliferation of HCV-infected cells but not of uninfected cells is highly sensitive to glutamine withdrawal

Huh7.5 cells were infected (MOI 1) and reseeded 5 dpi using the indicated conditioned cell media. Cell proliferation was monitored from the day of reseeding onwards (mean±SEM of one representative experiment of 4 performed with 6 biological replicates). **(A)** Cell proliferation count in the presence of conditioned media standardized to day 1 of reseeding; αKG (α-ketoglutarate; 2 mM). **(B)** Cell growth depicted in Figure 2A represented as area under curve (AUC) taking day 1 as baseline. **(C,D)** Viral infection at day 4 post-reseeding by IF using an anti-HCV serum and by HCV RTqPCR (standardized to replication in control medium).

Figure 4. Glutaminolyis is required for HCV replication

(A) Huh7.5 cells were infected with HCV (MOI 0.1). After 4 hrs culture media were replaced with conditioned media (control, no glutamine (gln), no gln + non-essential amino acids (NEAA), no gln + 2mM glutamate (glu), no gln + 2mM αKG). Intracellular HCV RNA levels were quantitated 3 dpi and standardized to infection in control medium. **(B)** shCTRL, shMYC and shGLS Huh7.5 cell lines (37, 38) were controlled for MYC and GLS silencing efficiencies and infected with HCV (MOI 0.1). 2mM αKG was added with the virus as indicated. Intracellular HCV RNA levels were measured by RT-qPCR 3 dpi. **(C)** Left graph: Viability was assessed in Huh7.5 cells by Neutral Red incorporation after 3 days

of treatment with MYC inhibitor 10058-F4 and GLS inhibitors BPTES and CB-839 at the indicated concentrations (μM). Middle/Right graphs: Huh7.5 cells were infected with HCV at the indicated MOIs. After 4 hrs cells were treated with vehicle (DMSO) or increasing concentrations of 10058-F4 (6.25, 12.5 and 25 μM), BPTES (1, 3 and 6 μM) and CB-839 (1, 5 and 10 μM). Intracellular HCV RNA levels were measured by RT-qPCR 3 dpi. DMSO volumes were the same for each drug condition. **(D)** Glutaminase inhibitor CB-839 was added at the indicated concentrations 4 hrs after infection (MOI 1) of Huh7.5 cells. The impact on HCV protein levels (representative western with anti-NS3 and NS5A antibodies), intracellular glutaminase activity (U/mg) and intracellular glutamate levels was assessed 3dpi. In the rightmost graph, 2mM αKG was added together with CB-839 to Huh7.5 cells 4 hrs after infection (MOI 1) and HCV replication levels were quantitated by RTqPCR at 3 dpi. **(E)** Persistently infected Huh7.5 cells (>10 days) were treated for 3 days with DMSO, 10058-F4 (12.5 and 25 μM) and CB-839 (1, 5 and 10 μM) and HCV replication quantitated by RT-qPCR and standardized to replication levels at the moment of addition of drugs. **(F)** Huh7.5 cells were infected with HCV (MOI 0.1) and treated with DMSO or 5 μM CB-839. 3 dpi superoxide anion levels were quantified by FACS using dihydroethidium (DHE). A representative FACS histogram is depicted. **(A-F)** Mean±SEM, n=minimum 3 experiments performed in triplicate.

Figure 5. Glutaminolytic factors are increased in liver biopsies of chronic hepatitis C patients and MYC, and SLC7A5 levels decrease with antiviral treatment

(A) *Top panel:* Transcript levels of MYC, SLC1A5, SLC7A5 and GLS were measured by RT-qPCR in liver biopsies of 119 HCV and 12 control patients. Min to max box plots of $2^{-\Delta Cp}$ values are shown. Statistics: Mann-Whitney U test. *Middle and bottom panel:* MYC, SLC1A5, SLC7A5 and GLS (KGA and GAC) transcript levels were plotted against activity grade (A1-A3) and fibrosis stage (F1-F4) of the chronic hepatitis C liver biopsies. Group sizes: Activity A1 n = 18; A2 n = 87; A3 n = 12; Fibrosis F1 n = 22; F2 n = 37; F3 n = 32; F4 = 10. Statistics: Mann-Whitney U test. **(B)** Transcript levels of HCV, MYC, SLC1A5, SLC7A5 and GLS were measured in 9 paired biopsies from chronic hepatitis C patients before and during/after interferon-α/ribavirin therapy. Results are presented as $2^{-\Delta Cp}$ values. Statistics: Wilcoxon signed rank test.

Figure 6. Glutamine is essential in many aspects of cell metabolism.

After entering the cell through specific transporters, glutamine (Gln) can be partially oxidized through glutaminolysis. The first and rate-limiting step is the conversion of glutamine to glutamate (Glu) by the enzyme glutaminase (GLS). Glu can then enter the TCA cycle after being converted to alpha-ketoglutarate (αKG). Gln is also a major precursor for nucleotide as well as glutathione (GSH) synthesis. ATP: adenosine triphosphate; Cit: citrate; Glc: glucose; Lac: lactate; Mal: malate; Pyr: pyruvate;

Acknowledgements

We thank H.GuillonAbiassi, L.Monnier, A.Roux, J.Lucifora for technical assistance and isolation of PHH, M. Rivoire for access to liver resections and S. Demo and Calithera Biosciences, Inc. for supplying CB-839 and helpful discussions.

Competing interest

The authors declare no competing interests.

Table 1. HCV alters amino acid levels in supernatants of infected cells. 3 dpi, supernatant of mock or infected cells was replaced with conditioned growth media (25mM glucose, 2mM glutamine; 25mM glucose; 2mM glutamine). 24hr later media were harvested and replaced. The procedure was repeated on day 4 and 5. Metabolites in supernatants were quantified by NMR. Values were corrected for metabolite concentration in the culture media not exposed to cells. Data (in arbitrary units) present the mean concentration measured days 3 to 5, corrected for cell density. Tendencies of metabolite concentrations to decrease or increase in infected cells are indicated by arrows. p values (Mann-Whitney U) are indicated. Statistically significant changes are marked in bold.

Metabolites (A.U.)	Glucose/Glutamine				Glucose only				Glutamine only			
	mock	HCV+		p value	mock	HCV+		p value	mock	HCV+		p value
Arg	-0,096	-0,069		0,2332	-0,208	-0,021		0,0420	-0,437	-1,230	↓	**0,0017**
Gln	-0,564	-0,709	↓	**0,0041**	-	-			-5,321	-7,832	↓	**0,0003**
Glt	0,063	0,508	↑	**0,0003**	0,061	0,234	↑	**0,0003**	0,202	1,771	↑	**0,0003**
Gly	-	-			-	-			0,320	0,862	↑	**0,0003**
Ile	-0,004	0,049		0,0851	0,187	0,158		0,4263	-0,042	-0,119		0,3311
His	-0,005	-0,024		0,2891	-0,043	0,015		0,0703	0,015	0,034		0,4529
Met	-0,042	0,056	↑	**0,0003**	0,005	0,024		0,0467	-0,217	-0,245		0,6911
Thr	-0,064	0,073	↑	**0,0469**	-0,057	0,189		0,0772	-0,041	-0,280	↓	**0,0041**
Tyr	0,038	0,050		0,3536	0,048	0,088		0,0849	0,130	0,089		0,5660
Val	-0,095	-0,142		0,0468	-0,213	-0,261		0,1451	-0,343	-0,766	↓	**0,0023**

Table 2. Spearman correlation analysis between MYC, SLC1A5, SLC7A5 and GLS (KGA and GAC) transcript levels and BMI score, alkaline phosphatase (AP), gamma glutamyl transferase (GGT), aspartate and alanine aminotransferase (ASAT, ALAT) and Albumin (Alb) levels and patients' age within the chronic hepatitis C cohort

		MYC	SLC1A5	SLC7A5	GLS KGA	GLS GAC
BMI	*r*	0.0512	0.1774	-0.0632	**0.3113**	**0.2553**
n=65	*p*	0.6905	0.1789	0.6201	**0.0138**	**0.0452**
AP	*r*	0.0951	0.0657	-0.1106	-0.0720	-0.1392
n=77	*p*	0.4171	0.5860	0.3450	0.5419	0.2368
GGT	*r*	0.0591	**0.2379**	-0.0541	**0.2294**	**0.2824**
n=78	*p*	0.6096	**0.0427**	0.6406	**0.0462**	**0.0141**
ASAT	*r*	**0.2692**	**0.2514**	0.1606	**0.3884**	**0.3951**
n=78	*p*	**0.0179**	**0.0319**	0.1630	**0.0005**	**0.0005**
ALAT	*r*	0.2174	0.2127	0.0290	0.2154	**0.2705**
n=78	*p*	0.0575	0.0708	0.8025	0.0616	**0.0189**
Alb	*r*	-0.2137	-0.0564	-0.1008	-0.1696	-0.0270
n=67	*p*	0.0825	0.6608	0.4206	0.1700	0.8312
Age	*r*	**0.2760**	**0.2970**	**0.2095**	**0.4830**	**0.3585**
n=90	*p*	**0.0092**	**0.0061**	**0.0487**	**<0.0001**	**0.0007**

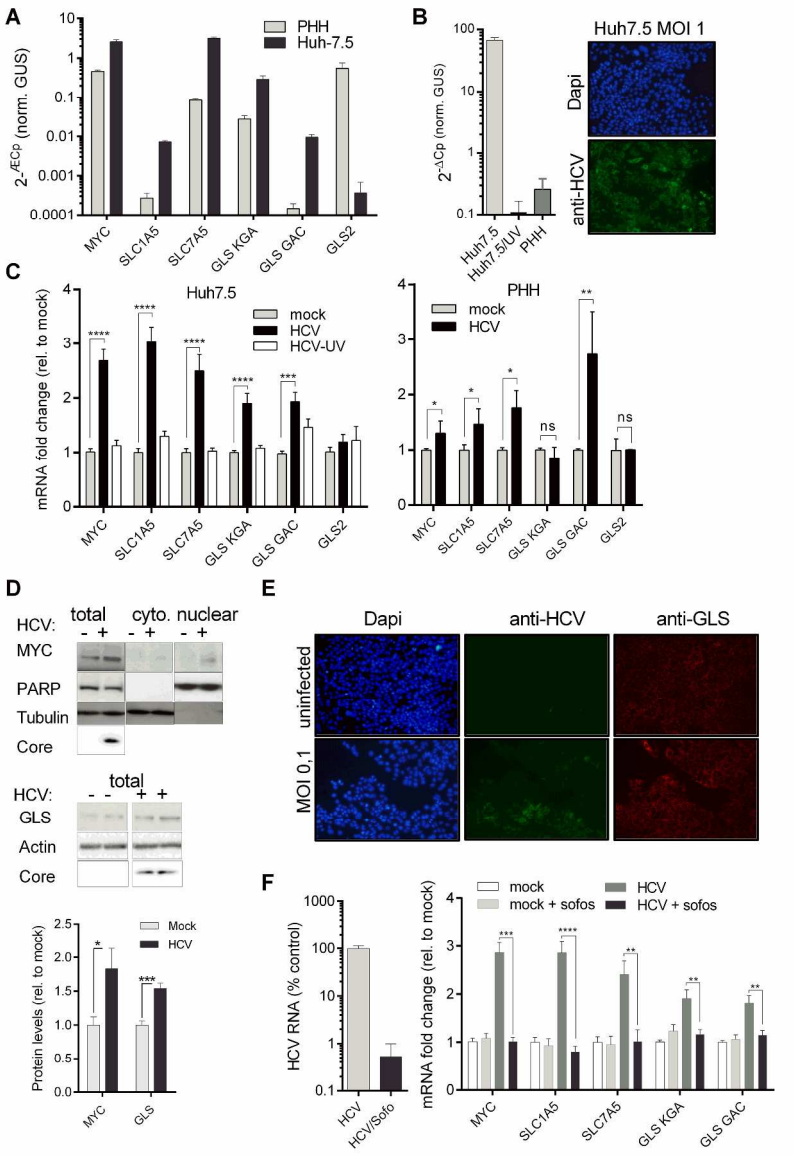

Figure 1. Glutaminolytic factors are increased in HCV-infected cells and return to basal levels upon viral clearance

(A) Expression levels of MYC, SLC1A5, SLC7A5 and GLS isoforms KGA and GAC or GLS2 transcripts were quantified by RT-qPCR in Huh7.5 cells and primary human hepatocytes (PHH) using GUS as housekeeping gene (mean±SEM values of 3 or more independent experiments). (B) HCV replication levels at 3 dpi in Huh7.5 cells infected (MOI 1) with native or UV irradiated virus analyzed by RTqPCR and immunofluorescence (IF) with an anti-HCV serum (green). PHH infected with HCV at an MOI of 5 to 10 and harvested between 3 and 5 dpi (absolute quantification revealed between 4000 to 9000 HCV genome copies/µg RNA). (C) MYC, SLC1A5, SLC7A5, GLS KGA /GAC and GLS2 transcript levels were amplified using GUS as housekeeping gene in Huh7.5 cells and PHH. Fold changes standardized to mock infection are shown (mean±SEM, n= 2 to 10 independent experiments). (D) Total lysates, nuclear and cytoplasmic fractions of HCV infected Huh7.5 cells were immunoblotted with -MYC, -PARP, -Tubulin, -GLS, -actin and -core specific antibodies. Protein quantification was performed with ImageJ software. Results were standardized to PARP

(MYC) or actin (GLS) expression and are expressed as fold change between infected and uninfected cells (a representative immunoblot is shown; graph: mean±SEM, n=4). (E) Huh7.5 cells were infected with HCV (MOI 0.1). 3 dpi, cells were fixed and stained with anti-HCV serum and anti-GLS antibody. Representative images are shown. (F) At 4 dpi infected (MOI 0,1) and uninfected Huh7.5 cells were treated with 5 µM sofosbuvir (Sofo) or carrier for 2 days. HCV, MYC, SLC1A5, SLC7A5 and GLS mRNA levels were quantified by RT-qPCR at 4 and 6 dpi using GUS as housekeeping gene. HCV data were standardized to infection at 4 dpi. MYC, SLC1A5, SLC7A5 and GLS were standardized to mock-infection (mean±SEM, n=up to 7) (C-F) Statistics: Student t-test.

301x443mm (300 x 300 DPI)

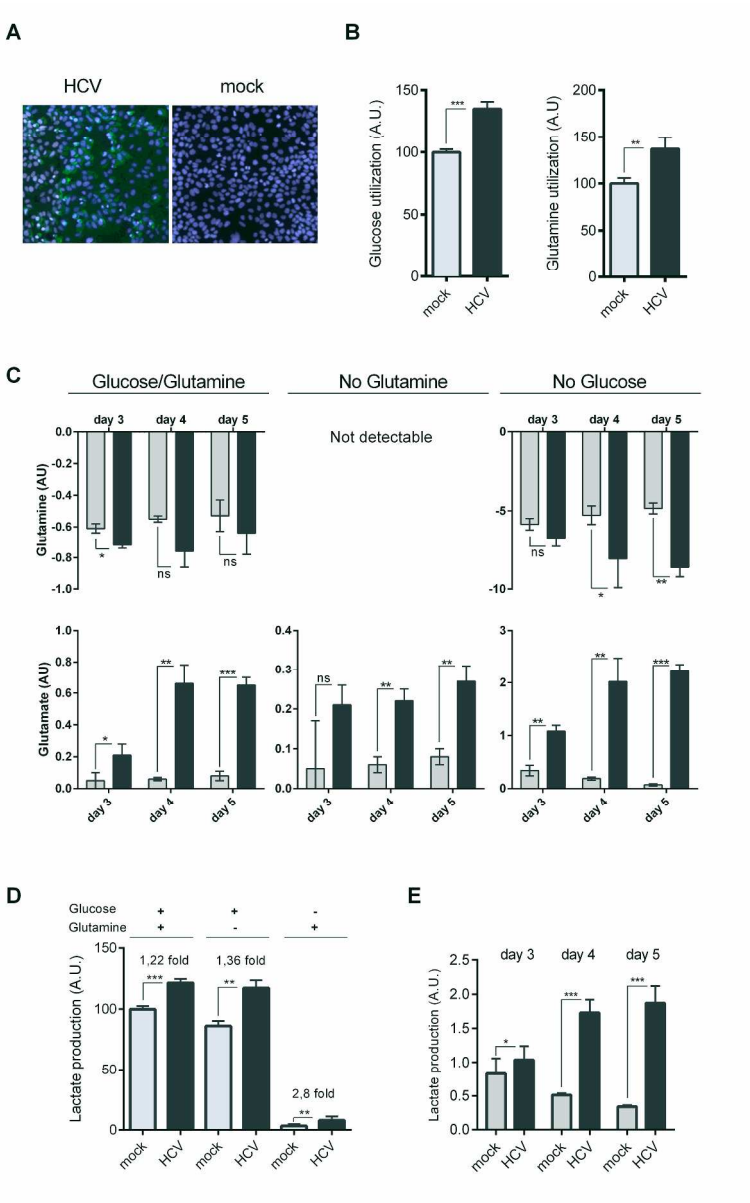

Figure 2. HCV infection increases glutamine utilization

(A–E) Huh7.5 cells were mock- or HCV-infected (MOI 1) for 3 days before cell media change. 24 hrs after the cell medium change, cell numbers were counted and supernatants harvested for metabolite quantification. Metabolite concentrations were corrected for cell numbers. Grey bars present mock, black bars HCV infected cultures. (A) HCV infection was controlled at 3 dpi by IF with an anti-HCV serum (green). (B) Glucose and glutamine consumption was measured biochemically in normal medium (25mM glucose, 2mM glutamine) and data were standardized to mock infected cells. (mean±SEM, n=4) (C) Supernatants of mock and infected cells cultured in normal medium or conditioned media containing only glucose or only glutamine were harvested 3, 4 and 5 dpi and subjected to NMR analysis. Glutamine and glutamate concentrations (arbitrary units) were standardized for cell numbers. (mean±STD, n=3). (D) Lactate was quantified biochemically in supernatants of infected/uninfected cells cultured in the indicated conditioned cell media at 3 dpi. Data are standardized to mock infected cells cultured in normal medium (mean±SEM, n=4). (E) Lactate was quantified by NMR in supernatants of mock and infected cells cultured in only glutamine

containing medium at 3, 4 and 5 dpi. Lactate concentrations (arbitrary units) were standardized for cell numbers. (mean±STD, n=3).

270x428mm (300 x 300 DPI)

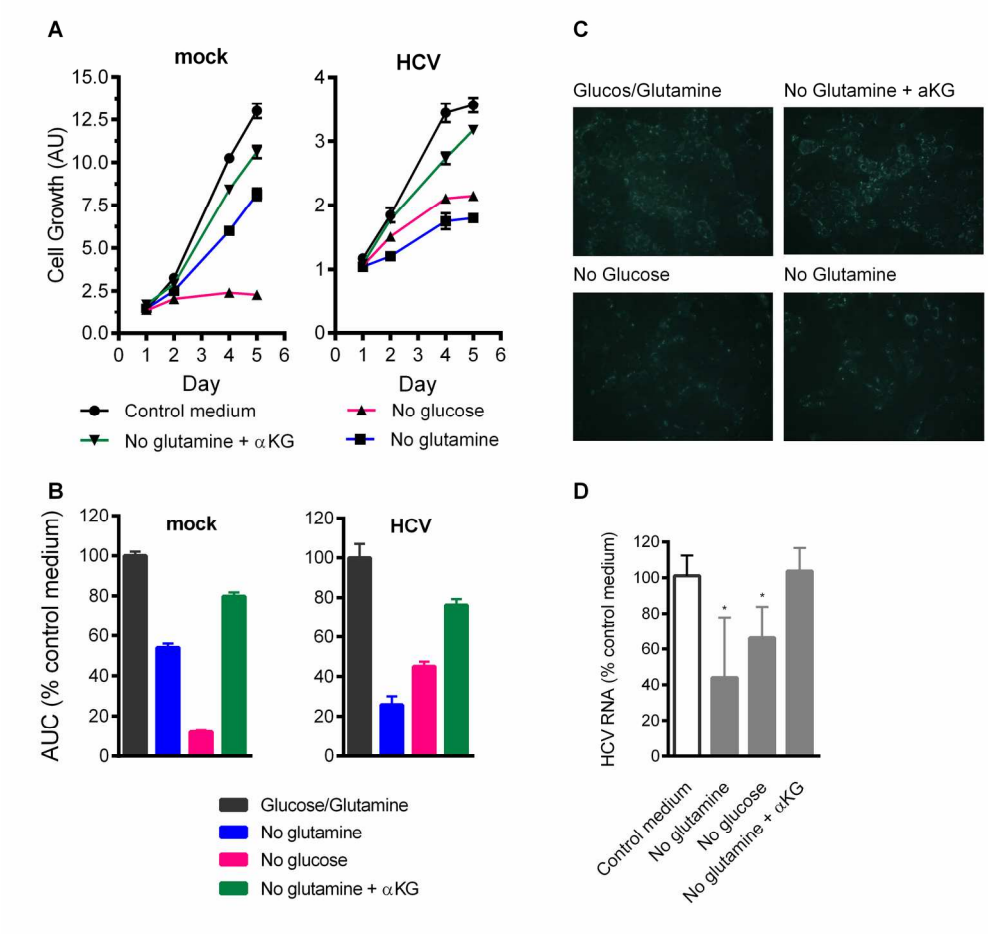

Figure 3. Proliferation of HCV-infected cells but not of uninfected cells is highly sensitive to glutamine withdrawal

Huh7.5 cells were infected (MOI 1) and reseeded 5 dpi using the indicated conditioned cell media. Cell proliferation was monitored from the day of reseeding onwards (mean±SEM of one representative experiment of 4 performed with 6 biological replicates). (A) Cell proliferation count in the presence of conditioned media standardized to day 1 of reseeding; αKG (α-ketoglutarate; 2 mM). (B) Cell growth depicted in Figure 2A represented as area under curve (AUC) taking day 1 as baseline. (C,D) Viral infection at day 4 post-reseeding by IF using an anti-HCV serum and by HCV RTqPCR (standardized to replication in control medium).

179x167mm (300 x 300 DPI)

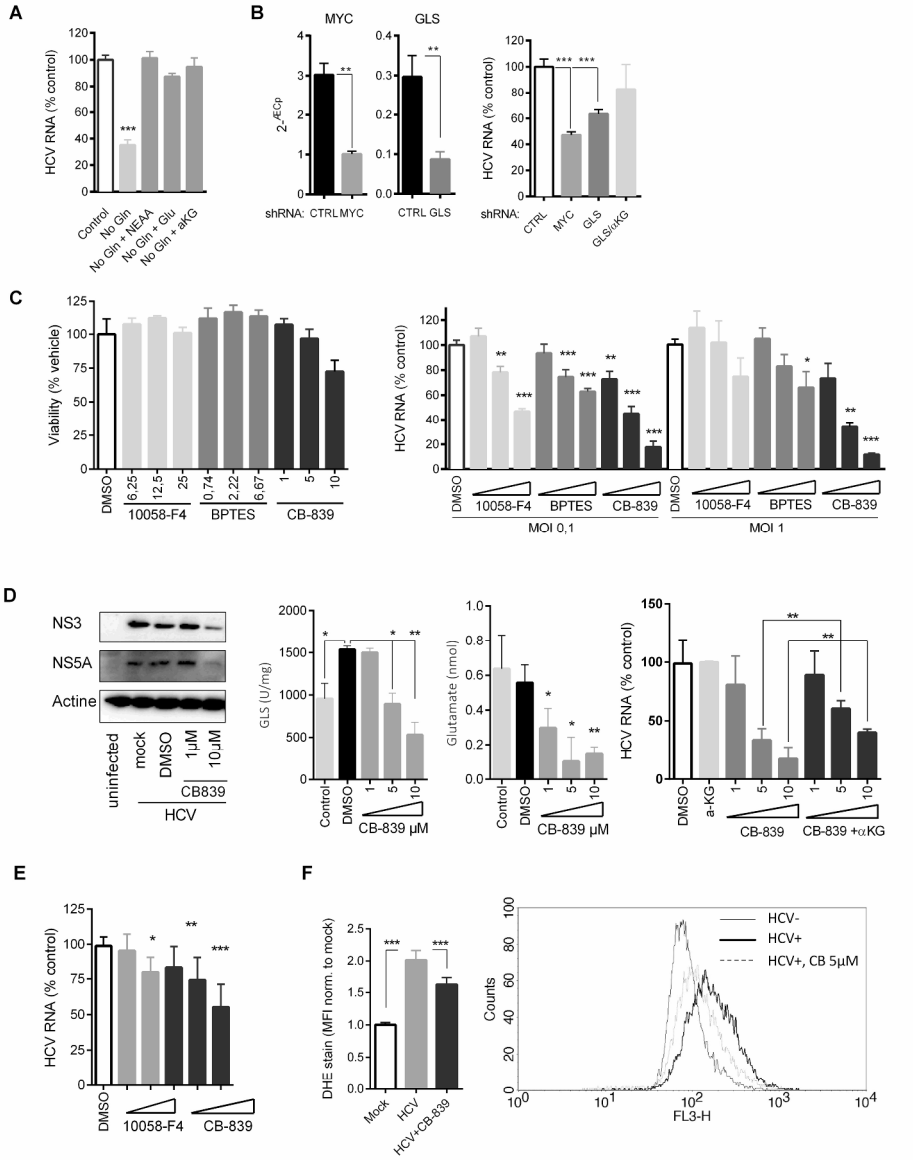

Figure 4. Glutaminolyis is required for HCV replication

(A) Huh7.5 cells were infected with HCV (MOI 0.1). After 4 hrs culture media were replaced with conditioned media (control, no glutamine (gln), no gln + non-essential amino acids (NEAA), no gln + 2mM glutamate (glu), no gln + 2mM αKG). Intracellular HCV RNA levels were quantitated 3 dpi and standardized to infection in control medium. (B) shCTRL, shMYC and shGLS Huh7.5 cell lines (37, 38) were controlled for MYC and GLS silencing efficiencies and infected with HCV (MOI 0.1). 2mM αKG was added with the virus as indicated. Intracellular HCV RNA levels were measured by RT-qPCR 3 dpi. (C) Left graph: Viability was assessed in Huh7.5 cells by Neutral Red incorporation after 3 days of treatment with MYC inhibitor 10058-F4 and GLS inhibitors BPTES and CB-839 at the indicated concentrations (µM). Middle/Right graphs: Huh7.5 cells were infected with HCV at the indicated MOIs. After 4 hrs cells were treated with vehicle (DMSO) or increasing concentrations of 10058-F4 (6.25, 12.5 and 25 µM), BPTES (1, 3 and 6 µM) and CB-839 (1, 5 and 10 µM). Intracellular HCV RNA levels were measured by RT-qPCR 3 dpi. DMSO volumes were the same for each drug condition. (D) Glutaminase inhibitor CB-839 was added at the indicated concentrations 4 hrs after infection

(MOI 1) of Huh7.5 cells. The impact on HCV protein levels (representative western with anti-NS3 and NS5A antibodies), intracellular glutaminase activity (U/mg) and intracellular glutamate levels was assessed 3dpi. In the rightmost graph, 2mM αKG was added together with CB-839 to Huh7.5 cells 4 hrs after infection (MOI 1) and HCV replication levels were quantitated by RTqPCR at 3 dpi. (E) Persistently infected Huh7.5 cells (>10 days) were treated for 3 days with DMSO, 10058-F4 (12.5 and 25 μM) and CB-839 (1, 5 and 10 μM) and HCV replication quantitated by RT-qPCR and standardized to replication levels at the moment of addition of drugs. (F) Huh7.5 cells were infected with HCV (MOI 0.1) and treated with DMSO or 5 μM CB-839. 3 dpi superoxide anion levels were quantified by FACS using dihydroethidium (DHE). A representative FACS histogram is depicted. (A-F) Mean±SEM, n=minimum 3 experiments performed in triplicate.

266x343mm (300 x 300 DPI)

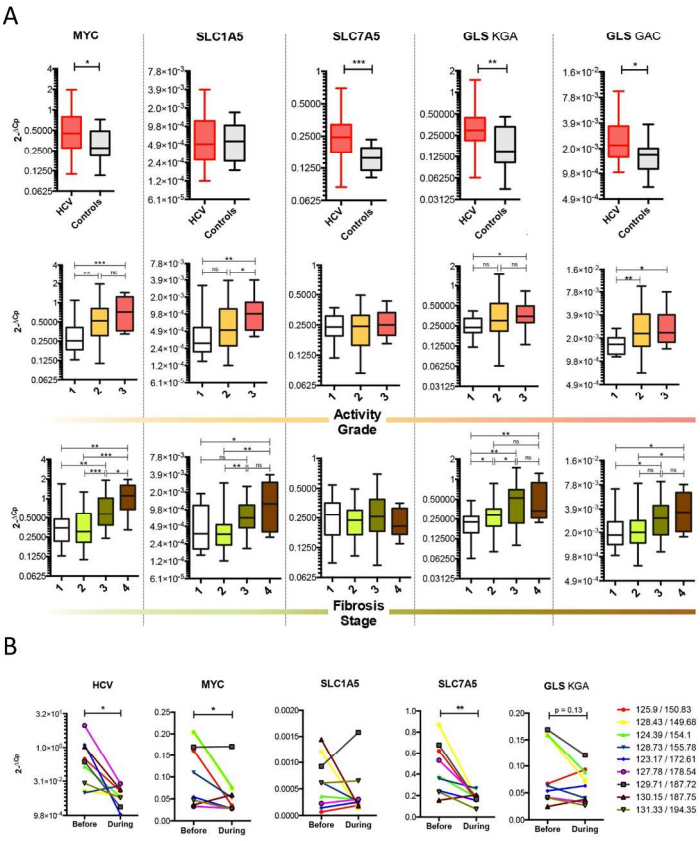

Figure 5. Glutaminolytic factors are increased in liver biopsies of chronic hepatitis C patients and MYC, and SLC7A5 levels decrease with antiviral treatment

(A) Top panel: Transcript levels of MYC, SLC1A5, SLC7A5 and GLS were measured by RT-qPCR in liver biopsies of 119 HCV and 12 control patients. Min to max box plots of 2-ΔCp values are shown. Statistics: Mann-Whitney U test. Middle and bottom panel: MYC, SLC1A5, SLC7A5 and GLS (KGA and GAC) transcript levels were plotted against activity grade (A1-A3) and fibrosis stage (F1-F4) of the chronic hepatitis C liver biopsies. Group sizes: Activity A1 n = 18; A2 n = 87; A3 n = 12; Fibrosis F1 n = 22; F2 n = 37; F3 n = 32; F4 = 10. Statistics: Mann-Whitney U test. (B) Transcript levels of HCV, MYC, SLC1A5, SLC7A5 and GLS were measured in 9 paired biopsies from chronic hepatitis C patients before and during/after interferon-α/ribavirin therapy. Results are presented as 2-ΔCp values. Statistics: Wilcoxon signed rank test.

190x275mm (300 x 300 DPI)

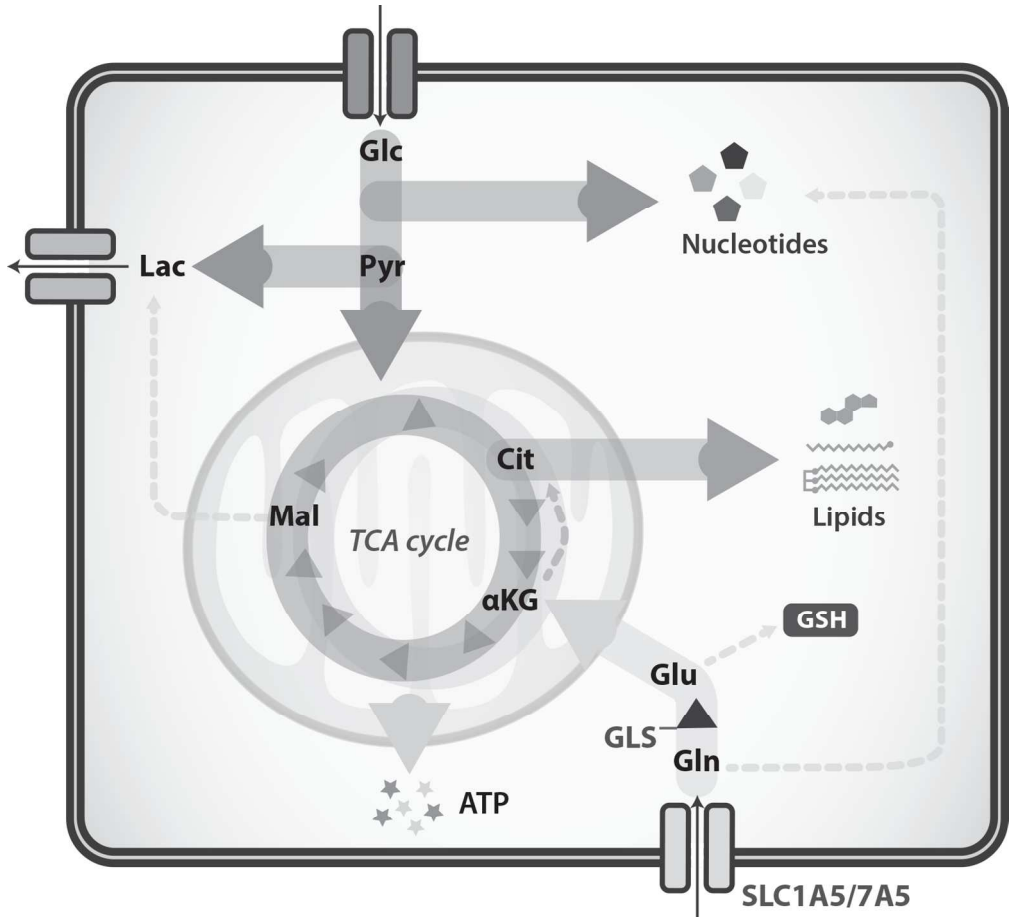

Figure 6. Glutamine is essential in many aspects of cell metabolism.
After entering the cell through specific transporters, glutamine (Gln) can be partially oxidized through glutaminolysis. The first and rate-limiting step is the conversion of glutamine to glutamate (Glu) by the enzyme glutaminase (GLS). Glu can then enter the TCA cycle after being converted to alpha-ketoglutarate (αKG). Gln is also a major precursor for nucleotide as well as glutathione (GSH) synthesis. ATP: adenosine triphosphate; Cit: citrate; Glc: glucose; Lac: lactate; Mal: malate; Pyr: pyruvate;

136x124mm (300 x 300 DPI)

Supplementary Experimental Procedures

Reagents

Sofosbuvir (Gilead), BPTES (Atlanchim Pharma), CB-839 (Calithera Biosciences, Inc.), 10058-F4 (Sigma), doxycycline (Sigma), dimethyl-2-oxoglutarate (Sigma), non-essential amino acids (Life Technologies), glutamic acid (Sigma).

Primary Human Hepatocytes

Primary human hepatocytes (PHH) were isolated from liver resections and cultivated as described previously [1].

UV-irradiation

Viral supernatant was irradiated in a Spectrolinker XL1000 (Spectronic Corporation) at 6000 µJ/cm2.

Cell proliferation assays

Proliferation of Huh7.5 cells was quantified by neutral red uptake assay [2]. Cell culture medium was replaced with a medium containing 40 µg/ml neutral red dye (Sigma), 2 h later cells were washed (PBS) and neutral red destain solution (50% ethanol, 1% glacial acetic acid) added. Measure of the neutral red extracts at OD 540 nm is an indicator of cell proliferation. Results were confirmed by cell counting (Cedex XS analyzer; Roche).

Lentiviruses

pGIPZ-shRNA-Crtl and pGIPZ-shRNA-GLS [3] were kindly provided by R.DeBerardinis, UT Southwestern, Dallas, United States. pRetrosuper-MYC-shRNA was from Addgene (15662).

Immunoblotting

After quantification using BCA Protein Assay Reagent (Thermo Scientific), cell lysates (50 mM Tris-HCl, pH 7.5, 150 mM NaCl, 0.1% SDS, 1% NP40, 1% protease inhibitors) were denatured 5 min at 95°C in Laemmli buffer and separated/blotted using SDS-PAGE/nitrocellulose. GLS, MYC, PARP, tubulin and β-actin were revealed using a rabbit polyclonal anti-GLS(1) antibody (Sigma SAB2105954), the mouse monoclonal 9E10 anti-MYC antibody (Santa Cruz), mouse monoclonals against PARP, tubulin and anti-β-actin (Sigma), respectively. Anti-rabbit and anti-mouse antibodies

coupled to horseradish peroxidase (Sigma) were used to detect proteins by enhanced chemiluminescence (Thermo Pierce).

Immunofluorescence

HCV-infected Huh7.5 cells were fixed with methanol/acetone (1:1) and immunostained using a patient-derived human anti-serum against HCV, anti-GLS (ab156876, abcam) and an Alexa Fluor 488-coupled secondary antibody (Life Technologies). Nuclei were stained using DAPI (Sigma).

NMR

The ^{1}H NMR experiments were performed at an ambient temperature of 298K on a Bruker Avance II spectrometer operating at a resonance frequency of 400 MHz for 1H and equipped with a 5 mm ATM BBI probe with z-gradient. Spectra were acquired using a 1D Nuclear Overhauser Enhancement Spectroscopy sequence (NOESY) with water presaturation ("noesypr1d" from the Bruker pulse-program library). Each spectrum was acquired applying 128 transients, a spectral width of 4795.4 Hz, a data size of 64 K points, an acquisition time of 6.83 s, a relaxation delay of 6s, a noesy mixing time of 20 ms. Additional 2D 1H-1H-TOCSY were applied for peak assignments of the different cell media (data not shown). Spectral processing was performed using the Bruker Topspin software (version 3.1, patch level 6). The co-added free induction decays (FIDs) were exponentially weighted with a line broadening factor of 0.3 Hz, Fourier-transformed, and manually phase corrected to obtain the 1H NMR spectra. A home-written Matlab program (using MATLAB R2012a, Mathworks®) was used for bucketing and Probabilistic Quotient Normalization (PQN) of the data. Buckets from the control culture media were subtracted from the buckets of the supernatant spectra, and scaled to the number of cells in the cell medium at the harvest point. Statistical chemometric analysis was done using PLS-Toolbox 7.5.2 (Eigenvector Research, Inc.) and Excel 2010 (Microsoft).

Supplementary References

1. Brault C, Levy P, Duponchel S, Michelet M, Salle A, Pecheur EI, Plissonnier ML, Parent R, Vericel E, Ivanov AV, Demir M, Steffen HM, Odenthal M, Zoulim F, Bartosch B. Glutathione peroxidase 4 is reversibly induced by HCV to control lipid peroxidation and to increase virion infectivity. Gut 2016;65:144-54.
2. Repetto G, del Peso A, Zurita JL. Neutral red uptake assay for the estimation of cell viability/cytotoxicity. Nat Protoc 2008;3:1125-31.
3. Cheng T, Sudderth J, Yang C, Mullen AR, Jin ES, Mates JM, DeBerardinis RJ. Pyruvate carboxylase is required for glutamine-independent growth of tumor cells. Proc Natl Acad Sci U S A 2011;108:8674-9.